Journal of Materials Chemistry B

RSC Publishing

PAPER

View Article Online
View Journal | View Issue

Cite this: *J. Mater. Chem. B*, 2013, **1**, 6115

A targetable nanogenerator of nitric oxide for light-triggered cytotoxicity†

Liu Yang, Shuqi Wu, Bijuan Lin, Tianxun Huang, Xiaoping Chen, Xiaomei Yan and Shoufa Han*

Received 13th August 2013
Accepted 16th September 2013

DOI: 10.1039/c3tb21131b

www.rsc.org/MaterialsB

Nanoscale-vesicles that can target pathogens are valuable for biomedical applications. In this study, a photo-responsive nanogenerator of nitric oxide (NO) comprised of a hydrophobic core of 3-trifluoromethyl-4-nitroaniline (TFNA) and a hydrophilic shell of mannosylated poly[styrene-*alter*-(maleic acid)] was constructed to target and kill lectin-expressing cells. The release of NO from the nanogenerator (T@P-M) was effectively induced by luminol-derived chemiluminescence (CL), leading to high-efficiency killing of *Escherichia coli* (*E. coli*) treated with T@P-M. In addition, the uptake of T@P-M by Raw 264.7 macrophages was achieved by cell surface lectin-mediated endocytosis, enabling the intracellular release of NO from the internalized T@P-M upon the induction of extracellular chemiluminescence. Because *in vivo*-generated CL can overcome the limited penetration of exogenous light into biological tissues, T@P-M has potential uses as a targetable photo-activatable microbicide to combat pathogens bearing lectins or residing in macrophages.

Introduction

Pathogens threaten human health in various ways, including infections and food contamination. With the rise of antibiotic resistance, alternative approaches to target and kill pathogens are highly valuable. Biogenic nitric oxide (NO) is harnessed by host immune systems to combat various invading pathogens.[1] In addition, NO is a cell signaling molecule that mediates a number of biological events, such as inflammation and wound healing.[2] The myriad biological roles of NO have stimulated enormous interest in developing NO-releasing systems that could be used to target pathogens or defined physio-pathological sites.[3] The grafting of NO donors to nano-scaffolds is an attractive approach to construct novel NO-releasing systems. NO donors such as diazeniumdiolates and *S*-nitrosothiols have been integrated into diverse carriers ranging from proteins and dendrimers to silica.[3,4] However, sophisticated procedures are often needed to minimize premature NO release from the resultant vehicles in biological settings due to the inherent instability of the NO donors resulting from autolysis, liability to acidic pH, or *trans*-*S*-nitrosation.[5] Furthermore, it is difficult to construct stable NO delivery systems capable of targeting selected cell types in a biological context.

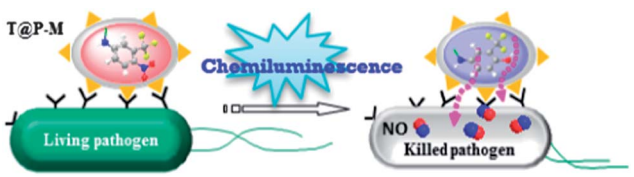

Fig. 1 Schematic of the antibacterial effects of T@P-M. Lectin–glycan interactions increase the local concentration of NO generated from the photo-activatable core.

Light is non-invasive and can be used to trigger the release of therapeutics in a spatiotemporally controlled manner. Apart from a few examples,[4e] the existing photo-responsive systems for NO release typically require the use of UV-vis light, which has limited penetration into biological tissues.[3,4] Chemiluminescence (CL) is biocompatible and could be generated within biological systems. Inspired by the potential of CL to overcome the limited penetration of exogenous light into biological tissues, we constructed a CL-responsive and targetable nanogenerator of NO (T@P-M) that is comprised of a hydrophobic core of 3-trifluoromethyl-4-nitroaniline (TFNA) and a hydrophilic shell of poly(styrene-*alter*-maleic acid) with multivalent mannose moieties. Cytotoxicity to lectin-expressing cells is achieved *via* CL-triggered NO release from TFNA encapsulated in T@P-M, which selectively binds *E. coli* or macrophages *via* multivalent cell surface lectin–glycan interactions (Fig. 1).

Results and discussion

Construction and characterization of T@P-M

Because NO-releasing systems that can be enriched at defined biological sites have not been extensively investigated, we

Department of Chemical Biology, College of Chemistry and Chemical Engineering, The Key Laboratory for Chemical Biology of Fujian Province, and The MOE Key Laboratory of Spectrochemical Analysis & Instrumentation, Xiamen University, Xiamen, China. E-mail: shoufa@xmu.edu.cn; Tel: +86-0592-2181728

† Electronic supplementary information (ESI) available: Analysis of T@P-M with cell surface lectins by confocal fluorescence microscopy. See DOI: 10.1039/c3tb21131b

sought to fabricate a targetable nano-vector using chemically glycosylated poly(styrene-*alter*-maleic acid) as the targetable carrier of TFNA, which is a NO photo-donor with high chemical stability under physiological conditions.[6] It is noteworthy that poly(styrene-*alter*-maleic acid) has low *in vivo* toxicity, and its conjugate with neocarcinostatin has been marketed for the treatment of hepatomas in Japan.[7] Briefly, poly(styrene-*alter*-maleic anhydride) (MW 20 000) partially conjugated with α-1-O-(2′-aminoethyl)-D-mannopyranoside (AE-MAN)[8] was fully amidated with TFNA in dimethylformamide (DMF) in the presence of triethylamine. The solution was extensively dialyzed against distilled water and then sonicated to afford T@P-M (Scheme 1). The infrared spectrum (IR) of lyophilized T@P-M had the characteristic peaks of TFNA (3370 cm^{-1}), demonstrating the successful incorporation of TFNA into the as-prepared T@P-M (Fig. S1, ESI†). Dynamic light scattering analysis showed that the statistical mean diameter of T@P-M dispersed in water was approximately 100 nm (Fig. 3). In contrast, no nanoscale particles were identified in the solution of mannosylated poly[styrene-*alter*-(maleic acid)], which was devoid of TFNA moieties (Fig. S3, ESI†), implying that the assembly of T@P-M into polymeric particles in aqueous solutions originated from the hydrophobic interactions of the pendant TFNA moieties.

Previously developed photo-responsive systems often rely on the use of external light for excitation.[3a] CL derived from luminol/horseradish peroxidase (HRP)/H_2O_2 is biocompatible and can be generated in the vicinity of acceptors in a biological context, *e.g.*, in wounds. To overcome the limited penetration of exogenous light into biological specimens, luminol-derived CL was employed as an internal molecular light source to activate T@P-M. As shown in Fig. 2A, TFNA and T@P-M both exhibit maximal absorption at 380 nm, which overlaps significantly with the light emission spectrum of CL, suggesting that CL resonance energy transfer (CRET) to T@P-M is feasible. To verify the CRET process, the luminol-derived CL intensity in phosphate-buffered saline (PBS) spiked with various levels of T@P-M was recorded, and the detected CL intensity decreased

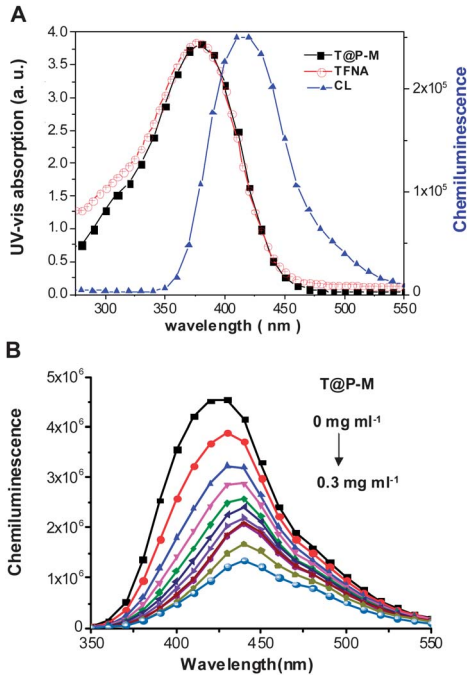

Fig. 2 CRET from the luminol-derived CL to T@P-M. (A) Absorption spectra of T@P-M and TFNA in PBS and the CL spectrum of luminol-derived CL in PBS. (B) CL emission intensity in PBS containing various concentrations of T@P-M. CL was triggered by the addition of H_2O_2 to PBS containing luminol (0.5 mM), 4-iodophenol (1 mM), and HRP (12 μg ml^{-1}) to a final concentration of 0.4 mM.

as a function of the T@P-M concentration, validating efficient CRET to T@P-M (Fig. 2B).

Next, we sought to determine whether the absorption of CL-generated light by T@P-M could result in effective NO release. Because *in situ*-generated NO can be oxidized to nitrate by H_2O_2 in the assay solution, nitroreductase was added to the T@P-M solution after CL illumination to convert the nitrate into nitrite, which was then quantitated using the Griess assay.[9] The nitrite concentration was 94 ± 0.8 μM in the solution of T@P-M (8 mg ml^{-1}) after 5 min of illumination. The level of nitrite produced is an indicator of the efficiency of CL-mediated NO release from T@P-M. Based on the quantity of TFNA encapsulated in T@P-M, the release efficiency was estimated to be 18%. Compared with previously developed systems,[10] our system has enhanced CRET

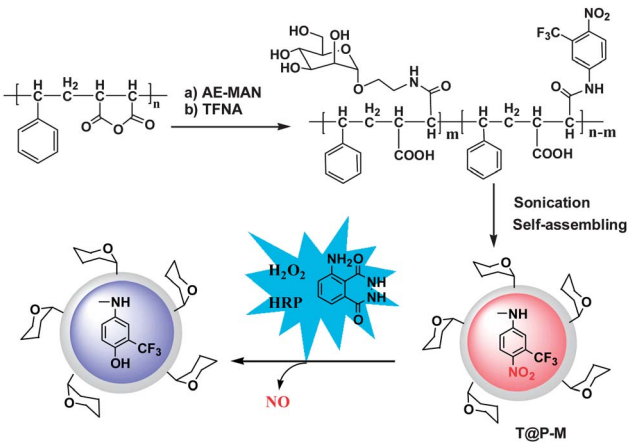

Scheme 1 Construction of mannose-displaying T@P-M and CL-mediated NO release from the encapsulated TFNA.

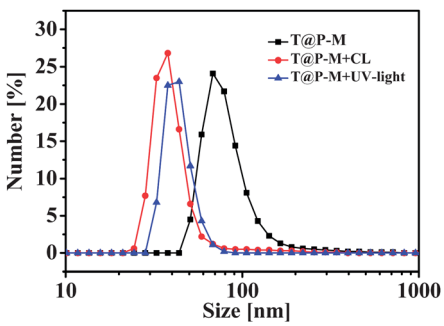

Fig. 3 Dynamic light scattering analysis of T@P-M before and after illumination with CL for 5 min in PBS.

efficiency, presumably due to the broad overlap of the CL spectrum (420 nm) with the absorption spectrum of T@P-M (Fig. 2B). Dynamic light scattering analysis showed that the mean diameter of T@P-M decreased markedly after CL illumination (Fig. 3), presumably due to the conversion of TFNA into hydrophilic phenolic products concomitant with NO release (Scheme 1).

Interaction of T@P-M with lectin-expressing cells

Lectins, glycan-binding proteins, are often expressed in unique patterns by defined cell lines and infectious microorganisms.[11] For instance, mannose-binding lectins are abundantly expressed on the cell surfaces of *E. coli* and macrophages.[12] As cell surface protein–glycan interactions mediate a large number of biological processes, *e.g.*, viral and bacterial infections, significant efforts have been devoted to the development of lectin-binding probes to inhibit infection by disrupting the natural glycan–lectin interactions at the interface between host cells and pathogens.[13]

To improve this strategy further, we employed lectin/T@P-M interactions to enhance the local concentration of antibacterial NO, the production of which from the cell-bound T@P-M could be photo-induced. Shown to be responsive to CL, T@P-M was evaluated to determine its ability to bind to *E. coli*. Confocal microscopy analysis of *E. coli* incubated with fluorescein-labeled T@P-M revealed significant fluorescence from the cells. In contrast, no fluorescence signal was found from *E. coli* treated with fluorescein-labeled T@P that lacked the mannose ligands (Fig. 4). The mannose-dependent staining of *E. coli* confirmed the critical role of the mannose moieties of T@P-M in the proposed glycan–lectin interactions.

The Raw 264.7 cell line is a mouse leukemic monocyte macrophage cell line with abundant mannose-specific lectins on the cell surface, and the CEM cell line is a T lymphocytic leukemia cell line that lacks mannose-binding lectins.[12d,12e] To determine if T@P-M could recognize lectins expressed on mammalian cells, Raw 264.7 cells and CEM cells were independently incubated with fluorescein-labeled T@P-M for 1 h at 4 °C to prevent non-specific endocytosis and then visualized by fluorescence confocal microscopy. As shown in Fig. 5, fluorescein fluorescence was clearly present on the periphery of the Raw 264.7 cells, whereas no fluorescence was observed on the CEM cells.

In previous studies, small-molecule NO donors immobilized on cationic scaffolds displayed enhanced antibacterial efficacy relative to free NO donors.[14] The improved antibacterial effects are attributed to the higher local NO concentrations conferred by the electrostatic interactions between the cationic scaffolds and the negatively charged cell membrane.[14] T@P-M exhibited a zeta potential of −34 mV under physiological conditions due to the presence of carboxylates (Fig. S2, ESI†). In contrast to these cationic NO-releasing systems, T@P-M is anionic and is anticipated to exhibit limited non-specific binding to lectin-free mammalian cells. Consistent with this hypothesis, low levels of T@P-M were observed on CEM cells (Fig. 5). The staining of *E. coli* and macrophages demonstrated the effectiveness of the targeting of cell surface mannose-binding lectins by T@P-M.

Chemiluminescence triggered cytotoxicity of T@P-M on *E. coli*

Shown to bind cell-surface lectins, T@P-M was further evaluated for its CL-mediated antibacterial effects. As shown in Fig. 6, the viability of *E. coli* treated with T@P-M and CL dramatically decreased, whereas the viability of the control cells treated with T@P-M or CL remained largely unaffected, demonstrating the CL-mediated bactericidal activity of T@P-M. As expected, no detrimental effects on the cell viability were observed for *E. coli* treated with T@P in the absence or presence of CL (Fig. 6). *Staphyloccocus aureus* is a Gram positive pathogen and is devoid of cell surface mannose-binding lectins. In contrast to the T@P-M dependent cytotoxicity to *E. coli*, no obvious influence could be identified on the viability of *Staphyloccocus aureus* treated with or without T@P-M in the presence of CL (Fig. S5, ESI†). Taken together, these results demonstrate the essential role of mannose–lectin interactions in the high specificity of the CL-mediated NO cytotoxicity to targeted *E. coli.*

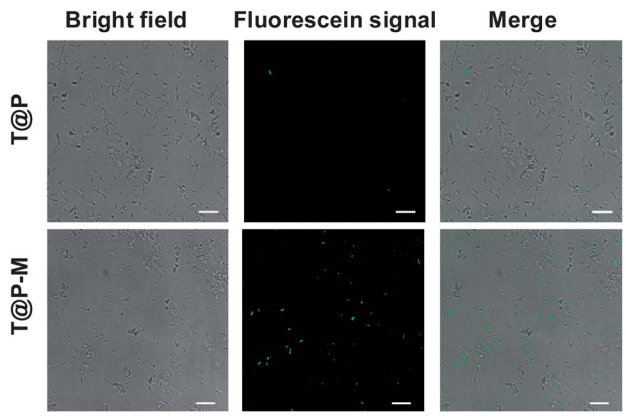

Fig. 4 Mannose-dependent binding of T@P-M to *E. coli*. *E. coli* were incubated with fluorescein-labeled T@P-M (0.5 mg ml^{-1}) or fluorescein-labeled T@P (0.5 mg ml^{-1}) in PBS at 4 °C for 1 h. The cells were washed with cold PBS and then visualized by fluorescence microscopy (λ_{ex}@488 nm). Bar: 5 μm.

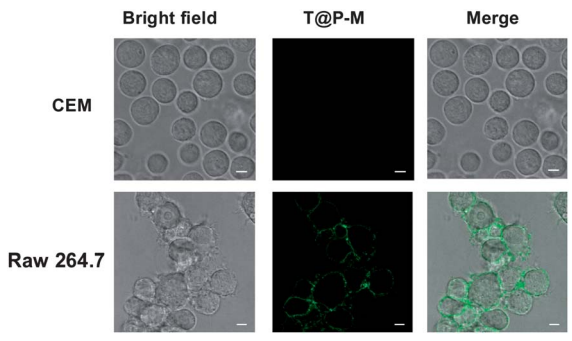

Fig. 5 Lectin-mediated binding of T@P-M to Raw 264.7 cells. Raw 264.7 cells and CEM cells were incubated with fluorescein-labeled T@P-M (0.5 mg ml^{-1}) at 4 °C for 1 h. The cells were rinsed with cold PBS to remove the unbound T@P-M and then analyzed by confocal fluorescence microscopy (λ_{ex}@488 nm). Bar: 5 μm.

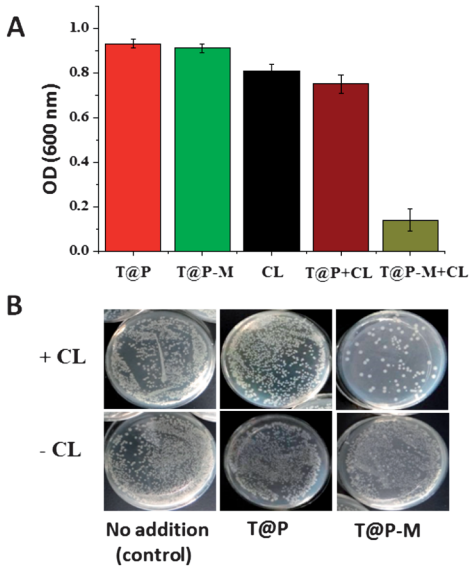

Fig. 6 CL-mediated antibacterial effects of T@P-M. *E. coli* were incubated for 30 min in PBS alone or PBS spiked with T@P (8 mg ml^{-1}) or T@P-M (8 mg ml^{-1}) and then illuminated with CL for 5 min. The cells were isolated and then cultured in LB medium at 37 °C for 24 h. The OD_{600} values of these cell suspensions were measured. (A). Alternatively, the treated cells were spread on agarose plates that were then incubated at 37 °C overnight and photographed (B).

Lectin mediated internalization of T@P-M into macrophages

To expand the therapeutic scope of T@P-M, fluorescein-labeled T@P-M was added to DMEM containing Raw 264.7 cells or RPMI-1640 containing CEM cells. The cells were cultured at 37 °C for 2 h and then stained with LysoTracker Red in DMEM or RPMI-1640 for 30 min. As shown in Fig. 7, no fluorescein fluorescence was observed inside the CEM cells, whereas intense fluorescein signals were observed within the Raw 264.7 cells. The colocalization of the intracellular fluorescein signals with the signals for LysoTracker Red, which is a lysosome-specific dye, indicates that T@P-M could be internalized into the lysosomes of mammalian cells *via* cell surface lectin-mediated endocytosis.

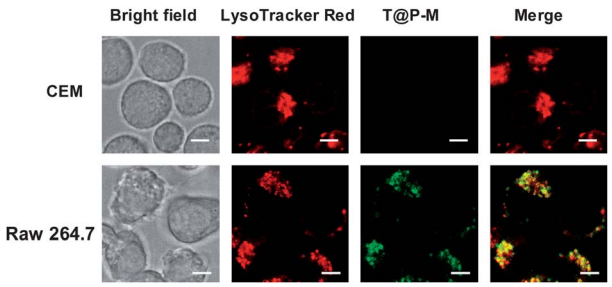

Fig. 7 Uptake of T@P-M by Raw 264.7 macrophages. CEM and Raw 264.7 cells were incubated with fluorescein-labeled T@P-M (0.5 mg ml^{-1}) for 2 h in DMEM or RPMI-1640. The cells were washed with PBS, cultured in DMEM or RPMI-1640 at 37 °C for 2 h, and then stained with LysoTracker Red (1 μM) in DMEM or RPMI-1640 for 30 min. The cells were analyzed by confocal fluorescence microscopy to probe the intracellular distribution of T@P-M. The merge of LysoTracker Red (shown in red) and T@P-M (shown in green) images demonstrated colocalization, indicated by the yellow areas. Bars, 5 μm.

Chemiluminescence mediated intracellular NO release from the internalized T@P-M in macrophages

To determine if T@P-M internalized by cells could be activated by extracellular CL, Raw 264.7 cells and CEM cells pre-loaded with T@P-M were stained with NO_{550}, a fluorogenic probe specific for intracellular NO,[15] and then exposed to CL or sodium nitroprusside (SNP), which is a widely used NO donor in cell biology studies. As expected, CEM cells and Raw 264.7 cells stained with NO_{550} exhibited intense intracellular fluorescence in the presence of SNP (Fig. 8). As shown in Fig. 8A, no fluorescence was observed in CEM cells treated with T@P-M and CL, suggesting that no detectable NO was photo-generated within CEM cells, which is consistent with the aforementioned observation that no T@P-M was internalized into CEM cells (Fig. 7). In contrast to CEM cells, Raw 264.7 cells treated with T@P-M and CL exhibited punctate fluorescence, indicative of extracellular CL-triggered NO release from the internalized T@P-M. Taken together, the bioimaging studies indicate that T@P-M can effectively bind to lectins on Raw 264.7 cells, can be internalized into these cells by lectin-mediated endocytosis, and can then be effectively activated by extracellular CL to produce NO within cells.

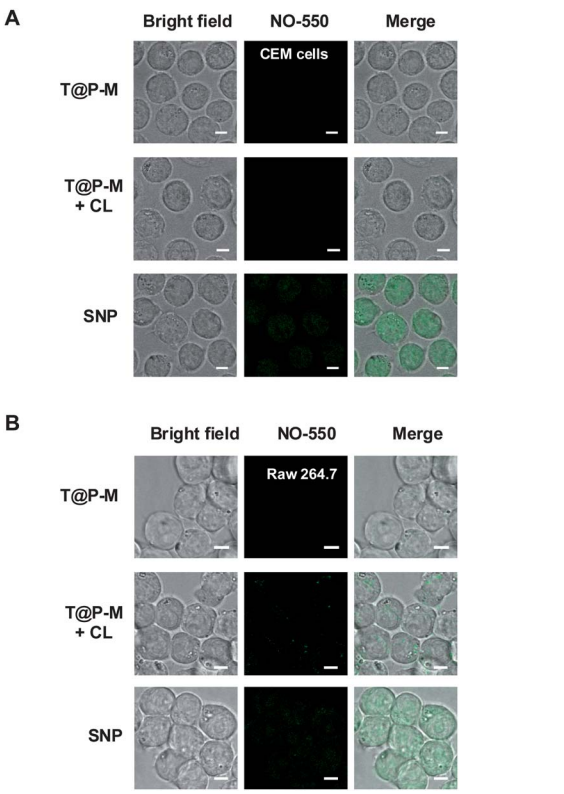

Fig. 8 Imaging of NO released from T@P-M in Raw 264.7 cells. CEM and Raw 264.7 cells preloaded with T@P-M (8 mg ml^{-1}) were washed with PBS and then cultured in DMEM or RPMI-1640 spiked with NO-550 (20 μM) at 37 °C for 20 min. The cells were washed and then incubated in PBS containing SNP (1 mM) for 15 min or incubated for 5 min in PBS containing luminol (0.5 mM), 4-iodophenol (1 mM), H_2O_2 (0.4 mM) and HRP (12 μg ml^{-1}). The cells were isolated and then imaged by fluorescence microscopy using an excitation wavelength of 476 nm.

After CL-triggered NO release from T@P-M within Raw 264.7 cells had been demonstrated, the cytotoxicity of the intracellularly released NO was determined by the MTT assay. As shown in Fig. 9, the viability of Raw 264.7 cells treated with T@P-M was 94%, indicating that T@P-M has low cytotoxicity. Upon CL illumination, the viability of Raw 264.7 cells loaded with T@P-M decreased to 49%, whereas no effects were observed on CEM cells under identical assay conditions, demonstrating that the CL triggered NO production by the endocytosed T@P-M, resulting in cytotoxicity. In separate experiments, no cytotoxicity was observed for Raw 264.7 cells treated with TFNA, a small molecular NO donor, in the absence or presence of CL. The different toxic effects of T@P-M on CEM cells *vs.* Raw 264.7 cells further validated the cell surface lectin-dependent cellular uptake of T@P-M, which enabled CL-mediated cytotoxicity resulting from NO released from the internalized T@P-M.

The broad spectrum biocidal activity of NO has been ascribed to oxidative stress, caused by NO or reactive nitrogen species derived from NO, such as dinitrogen trioxide, to the targeted cells.[18] The oxidative stress alters the structures and functions of proteins, DNA, cell membranes, *etc.*, leading to cytotoxicity of NO treated pathogens or cancer cells. As a highly reactive free radical, NO is short lived and diffuses over a short distance due to the detoxification by off-target biomolecules. Therefore it is critical to administer NO in the proximity of the downstream targets. However, many systems use cationic vectors to electrostatically bind anionic pathogens to give enhanced local concentration of NO.[14] The cationic nature of these systems leads to compromised discrimination of pathogens from host cells. In contrast, T@P-M is negatively charged and exhibits minimal binding to lectin-negative host cells due to Coulombic repulsion with anionic cell surface constituents. The recruitment of T@P-M by lectins located on the target cells enables local release of NO upon light activation, which underlies the observed efficient killing of *E. coli* and macrophages.

In nature, macrophages capture and deliver pathogens into lysosomes for degradation. However, a number of pathogens, such as *Mycobacterium tuberculosis*, can effectively escape this pathway and replicate within macrophages in human hosts. The moderate cytotoxicity of T@P-M to Raw 264.7 cells suggests that T@P-M may have potential uses in combating macrophage-residing pathogens through the cell surface lectin-mediated enrichment of T@P-M in macrophages. In this system, the desired levels of intracellular NO might be achieved by the introduction of appropriate levels of T@P-M.

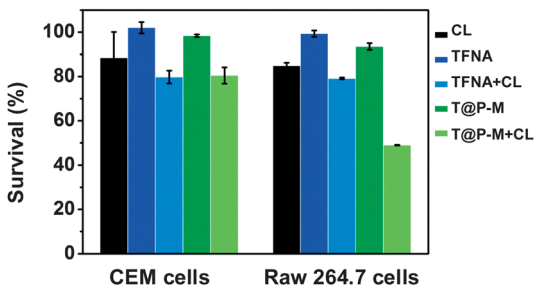

Fig. 9 CL-mediated cytotoxicity of T@P-M to Raw 264.7 cells. CEM cells and Raw 264.7 cells were cultured in RPMI-1640 or DMEM containing TFNA (0.52 mM) or T@P-M (8 mg ml^{-1}, with the same level of TFNA) for 20 min. The cells were washed and then subjected to CL for 5 min. The viability of the treated cells was determined by the MTT assay.

Conclusions

T@P-M with three structural elements, a biocompatible carrier composed of poly(styrene-*alter*-maleic acid), a photo-activatable NO-releasing core, and mannose ligands displayed on the shell, was successfully constructed for selective binding to cell surface lectins. Significant and lectin-dependent cell death was induced in *E. coli* and Raw 264.7 cells *via* NO released from T@P-M upon CL. In contrast to previous studies in which the cationic NO delivery systems non-specifically bound to anionic cell surfaces, the negatively charged T@P-M exhibits low-background binding to lectin-negative cells due to the Coulombic repulsion of anionic species located on mammalian cells, such as sialic acids. Most importantly, the responsiveness of T@P-M to CL, which could be generated *in vivo* and thus overcome the limited penetration of exogenous light into biological tissues, indicates that T@P-M has broad biomedical applications, *e.g.*, for combating pathogens with defined cell surface lectins in wounds or possibly pathogens residing in macrophages through host cell surface lectin-mediated enrichment of photo-toxic T@P-M.

Experimental

Material and methods

LysoTracker Red DND-99 was purchased from Invitrogen. 4′-(Aminomethyl)fluorescein and NO-550 were gifts from Bioluminor. α-1-*O*-(2′-Aminoethyl)-D-mannopyranoside was synthesized according to a reported procedure.[16] Poly[styrene-*alt*-(maleic anhydride)]$_{40}$ was prepared following a published method.[17] Unless specified, all other reagents were obtained from Alfa Aesar. IR spectra were obtained using KBr discs with a Nicolet 330 infrared spectrometer. Chemiluminescence emission spectra and UV-vis absorption spectra were recorded on a spectrofluorometer (SpectraMax M5, Molecular Device). CEM cells and Raw 264.7 cells were obtained from the American Type Culture Collection (ATCC). Confocal fluorescence microscopy images were obtained on a Leica SP5 using the following filters: λ_{ex}@476 nm and λ_{em}@500–580 nm for the NO-550 signal, λ_{ex}@488 nm and λ_{em}@500–530 nm for the fluorescein signal, and λ_{ex}@543 nm and λ_{em}@580–620 nm for the LysoTracker Red DND-99 signal. The fluorescence signals of LysoTracker Red and fluorescein inside cells were merged using Photoshop CS 5.0.

Preparation of T@P-M

A DMF solution (3 ml) containing *O*-(2′-aminoethyl)-D-mannopyranoside (0.2 g) and triethylamine (0.5 ml^{-1}) was added dropwise to a solution of poly(styrene-*alt*-MAA) (MW: 20 000) (1.0 g) in DMF (5 ml). The solution was stirred at rt for 30 min, and TFNA (0.8 g) was added. The solution was stirred at rt for 1 h, and then Na_2CO_3 (1.0 g) in distilled water (30 ml) was added. The mixture was stirred and sonicated at rt for 10 min and then extensively dialyzed against distilled water to afford T@P-M.

Preparation of fluorescein-labeled T@P-M

A DMF solution (3 ml) containing 4′-(aminomethyl)fluorescein (0.1 g), *O*-(2′-aminoethyl)-D-mannopyranoside (0.2 g), and TEA (0.5 ml) was added to a solution of poly(styrene-*alt*-MAA) (MW: 20 000) (1.0 g) in DMF (5 ml). The solution was stirred at rt for 30 min, and TFNA (0.8 g) was added. The solution was stirred at rt for 1 h, and then Na_2CO_3 (1.0 g) in distilled water (30 ml) was added. The mixture was stirred and sonicated at rt for 10 min and then extensively dialyzed against distilled water to afford fluorescein-labeled T@P-M.

Preparation of T@P

TFNA (0.8 g) and TEA (0.5 ml) were added to a DMF solution (5 ml) containing poly(styrene-*alt*-MAA) (1.0 g). The mixture was stirred at rt for 1 h, and then Na_2CO_3 (1.5 g) in water (30 ml) was added to the reaction mixture. The mixture was sonicated at rt for 10 min and then dialyzed against distilled water to afford T@P.

Preparation of fluorescein-labeled T@P

A DMF solution (3 ml) containing 4′-(aminomethyl)fluorescein (0.1 g) and TEA (0.5 ml) was added to a solution of poly(styrene-*alt*-MAA) (MW: 20 000) (1.0 g) in DMF (5 ml). The solution was stirred at rt for 30 min, and then TFNA (0.8 g) was added. The mixture was stirred at rt for 1 h, and then Na_2CO_3 (1.0 g) in distilled water (30 ml) was added. The mixture was sonicated and then extensively dialyzed against distilled water to afford fluorescein-labeled T @P.

FT-IR spectroscopy analysis

Well-ground TFNA (10 mg), freeze-dried T@P (10 mg), or freeze-dried T@P-M (10 mg) was placed between two KBr plates and dispersed with a gentle circular and back-and-forth rubbing motion of the plates. The samples were then analyzed using a Nicolet 330 infrared spectrometer.

Chemiluminescence system

The following conditions were employed for CL generation in this work: H_2O_2 was added to PBS containing luminol (0.5 mM), HRP (12 μg ml^{-1}), 4-iodophenol (1 mM), and the appropriate cell samples/polymeric nanoparticles to a final concentration of 0.4 mM to initiate CL. After 5 min of illumination after the addition of H_2O_2, the cells were harvested, washed with fresh PBS and then subjected to further analysis.

Dynamic size and zeta potential measurements

Freeze-dried T@P-M was dissolved in distilled water to a concentration of 4 mg ml^{-1}. The solution was sonicated and passed through a 0.4 μm filter. A portion of the filtered solution was illuminated for 1 h with a hand-held UV illuminator (365 nm). The T@P-M solutions treated with or without UV light were analyzed using a Zetasizer NaNO ZS (ZEN3500) to determine the statistical size distributions and zeta potentials.

Binding of T@P-M to cell surface lectins

E. coli cells were incubated with fluorescein-labeled T@P-M (8 mg ml^{-1}) or T@P (8 mg ml^{-1}) in PBS for 30 min. The cells were centrifuged, washed with PBS, and then re-suspended in PBS. The cells were visualized by fluorescence microscopy. In a separate experiment, Raw 264.7 cells and CEM cells were incubated with fluorescein-labeled T@P-M (8 mg ml^{-1}) in PBS at 4 °C for 1 h. The cells were washed with cold PBS and then analyzed using a confocal fluorescence microscope.

CL-mediated killing of *E. coli* with T@P-M

A single colony of kanamycin-resistant *E. coli* BL21(DE3) on a solid yeast-extract tryptone dextrose (YTD) agar plate was transferred to liquid YTD culture medium (6 ml) and then grown at 37 °C and 220 rpm overnight. The *E. coli* cells were harvested by centrifugation. The *E. coli* pellet was dispersed in PBS (10 mM, pH 7.4) and then centrifuged. The supernatant was discarded, and the pellet was re-suspended in PBS and then diluted to an optical density of 1.0 at 600 nm ($OD_{600} = 1.0$). The as-prepared *E. coli* samples (1 ml) were added to PBS spiked with T@P-M (8 mg ml^{-1}) or T@P (8 mg ml^{-1}) or un-spiked PBS. The mixtures were incubated for 30 min, and then, the cells were collected by centrifugation and washed with PBS. After the supernatant had been removed, the three cell populations were added to the aforementioned CL system. The three solutions were vortexed vigorously. Each solution was divided into two portions; water (control) was added to one portion, and H_2O_2 (0.4 mM) was added to the other. The reaction mixtures were incubated at rt for 5 min and then centrifuged to remove the supernatant.

The resultant *E. coli* samples were re-suspended in PBS (1 ml). A portion of each solution was immediately placed in LB medium (250-fold dilution) and cultured at 37 °C and 220 rpm. The optical densities of the LB media at 600 nm were measured after 8 h of incubation. In parallel, a portion of each treated *E. coli* samples was placed in LB medium (1000-fold dilution). After thorough mixing, 50 μl of each sample was spread on an agarose plate. The plates were incubated at 37 °C for 24 h. The plates were photographed, and the colonies were counted.

Effects of T@P-M on *Staphyloccocus aureus*

Staphyloccocus aureus cells were washed with PBS and the cell pellet was re-suspended in PBS and then diluted to an optical density of 1.0 at 600 nm ($OD_{600} = 1.0$). The resultant cell sample (1 ml) was respectively added to PBS spiked with or without T@P-M (8 mg ml^{-1}). The two mixtures were incubated for 30 min at rt and the cells were collected by centrifugation and then washed with PBS. The sample solutions were centrifuged and the cell pellets were added into the aforementioned CL system. The solutions were thoroughly mixed and then to the solutions was added H_2O_2 (0.4 mM). The reaction mixtures were incubated at rt for 5 min. The cells were harvested by centrifugation and then re-suspended in PBS (1 ml). The solutions were respectively diluted into LB medium (250-fold) and then cultured at 37 °C and 220 rpm. The optical densities of the LB

media at 600 nm were measured post 24 h incubation. In a parallel experiment, the cells treated with T@P-M in the absence of CL were cultured in the medium and used as the control.

Lectin-mediated internalization of T@P-M

Raw 264.7 cells and CEM cells were incubated in DMEM or RPMI-1640 supplemented with fluorescein-labeled T@P-M (0.5 mg ml^{-1}) at 37 °C for 2 h. The medium was removed, and the cells were washed twice with PBS. The cells were cultured in DMEM or RPMI-1640 at 37 °C for 2 h. The cells were then incubated in DMEM or RPMI-1640 containing LysoTracker Red (1 μM) for 30 min and analyzed by confocal fluorescence microscopy. The fluorescence emission of LysoTracker Red between 580 and 620 nm was recorded using an excitation wavelength of 543 nm. The fluorescence emission of fluorescein between 500 and 530 nm was recorded using an excitation wavelength of 488 nm.

Imaging of CL-triggered NO-release from T@P-M in macrophages

Raw 264.7 cells and CEM cells were incubated for 20 min at 37 °C in DMEM and RPMI-1640, respectively, containing T@P-M (8 mg ml^{-1}). The cells were washed with PBS and then cultured in DMEM or RPMI-1640 spiked with NO 550 (20 μM). The cells were harvested and then exposed to CL for 5 min in PBS. The cells were collected by centrifugation, washed with PBS and then analyzed by confocal fluorescence microscopy. The level of NO-mediated turn-on fluorescence between 500 and 580 nm was recorded using an excitation wavelength of 476 nm.

In control experiments, both cell types were incubated in DMEM or RPMI-1640 spiked with TFNA (0.107 mg ml^{-1}) for 20 min at 37 °C. The cells were washed with PBS and then cultured in DMEM or RPMI-1640 spiked with NO-550 (20 μM) at 37 °C for 20 min. The cells were washed, and then a portion of the cells was incubated for 5 min in PBS containing luminol (0.5 mM), 4-iodophenol (1 mM), H_2O_2 (0.4 mM) and HRP (12 μg ml^{-1}). The cell samples treated with or without CL were isolated and then imaged by fluorescence microscopy.

CL-mediated cytotoxicity of T@P-M to Raw 264.7 cells

Raw 264.7 and CEM cells were seeded in 96-well plates at a density of 1×10^5 cells per well and then incubated overnight in DMEM or RPMI-1640 containing 10% fetal bovine serum (FBS). The cells were washed with PBS and then incubated in fresh medium or RPMI-1640 containing TFNA (0.107 mg ml^{-1}) or T@P-M (8 mg ml^{-1}) for 20 min. The media were replaced with PBS containing CL reagents. After 5 min of CL illumination, the cells were incubated in DMEM containing tetrazolium dye (MTT) (0.25 mg ml^{-1}) and cultured for 4 h at 37 °C. After removal of the supernatant, DMSO (100 μl) was added to each well to dissolve the formazan crystals. The plates were shaken for 5 min and then analyzed with a SpectraMax M5 plate reader to record the absorbance at 490 nm.

Acknowledgements

This work was supported by grants from NSF China (no. 21305116, 21272196 and 21072162), 973 program 2013CB933901, PCSIRT, NFFTBS (no. J1310024), and the Fundamental Research Funds for the Central Universities 2011121020.

Notes and references

1 (*a*) S. Carlsson, E. Weitzberg, P. Wiklund and J. O. Lundberg, *Antimicrob. Agents Chemother.*, 2005, **49**, 2352; (*b*) D. Fukumura, S. Kashiwagi and R. K. Jain, *Nat. Rev. Cancer*, 2006, **6**, 521.

2 (*a*) R. F. Furchgott, *Angew. Chem., Int. Ed.*, 1999, **38**, 1870; (*b*) L. J. Ignarro, *Angew. Chem., Int. Ed.*, 1999, **38**, 1882; (*c*) F. Murad, *Angew. Chem., Int. Ed.*, 1999, **38**, 1857.

3 (*a*) S. Sortino, *Chem. Soc. Rev.*, 2010, **39**, 2903; (*b*) A. B. Seabra and N. Duran, *J. Mater. Chem.*, 2010, **20**, 1624.

4 (*a*) N. Kandoth, E. Vittorino and S. Sortino, *New J. Chem.*, 2011, **35**, 52; (*b*) E. B. Caruso, S. Petralia, S. Conoci, S. Giuffrida and S. Sortino, *J. Am. Chem. Soc.*, 2007, **129**, 480; (*c*) D. Neuman, A. D. Ostrowski, R. O. Absalonson, G. F. Strouse and P. C. Ford, *J. Am. Chem. Soc.*, 2007, **129**, 4146; (*d*) R. Etchenique, M. Furman and J. A. Olabe, *J. Am. Chem. Soc.*, 2000, **122**, 3967; (*e*) J. V. Garcia, J. Yang, D. Shen, C. Yao, X. Li, R. Wang, G. D. Stucky, D. Zhao, P. C. Ford and F. Zhang, *Small*, 2012, **8**, 3800; (*f*) A. R. Rothrock, R. L. Donkers and M. H. Schoenfisch, *J. Am. Chem. Soc.*, 2005, **127**, 9362; (*g*) N. A. Stasko and M. H. Schoenfisch, *J. Am. Chem. Soc.*, 2006, **128**, 8265; (*h*) H. Zhang, G. M. Annich, J. Miskulin, K. Stankiewicz, K. Osterholzer, S. I. Merz, R. H. Bartlett and M. E. Meyerhoff, *J. Am. Chem. Soc.*, 2003, **125**, 5015; (*i*) J. H. Shin, S. K. Metzger and M. H. Schoenfisch, *J. Am. Chem. Soc.*, 2007, **129**, 4612; (*j*) W. Cai, J. Wu, C. Xi and M. E. Meyerhoff, *Biomaterials*, 2012, **33**, 7933; (*k*) B. Sun, D. L. Slomberg, S. L. Chudasama, Y. Lu and M. H. Schoenfisch, *Biomacromolecules*, 2012, **13**, 3343; (*l*) Y. Lu, B. Sun, C. Li and M. H. Schoenfisch, *Chem. Mater.*, 2011, **23**, 4227; (*m*) D. A. Riccio and M. H. Schoenfisch, *Chem. Soc. Rev.*, 2012, **41**, 3731.

5 P. G. Wang, M. Xian, X. Tang, X. Wu, Z. Wen, T. Cai and A. J. Janczuk, *Chem. Rev.*, 2002, **102**, 1091.

6 (*a*) T. Suzuki, O. Nagae, Y. Kato, H. Nakagawa, K. Fukuhara and N. Miyata, *J. Am. Chem. Soc.*, 2005, **127**, 11720; (*b*) S. Sortino, G. Marconi and G. Condorelli, *Chem. Commun.*, 2001, 1226.

7 H. Maeda, *Adv. Drug Delivery Rev.*, 2001, **46**, 169.

8 R. Su, L. Li, X. Chen, J. Han and S. Han, *Org. Biomol. Chem.*, 2009, **7**, 2040.

9 J. B. J. Fox, *Anal. Biochem.*, 1979, **51**, 1493.

10 X. Liu, R. Freeman, E. Golub and I. Willner, *ACS Nano*, 2011, **5**, 7648.

11 B. E. Collins and J. C. Paulson, *Curr. Opin. Chem. Biol.*, 2004, **8**, 617.

12 (*a*) M. Slavikova, R. Lodinova-Zadnikova, I. Adlerberth, L. A. Hanson, C. Svanborg and A. E. Wold, *Adv. Exp. Med. Biol.*, 1995, **371A**, 421; (*b*) Y. Eshdat, I. Ofek, Y. Yashouv-Gan,

N. Sharon and D. Mirelman, *Biochem. Biophys. Res. Commun.*, 1978, **85**, 1551; (*c*) I. Ofek, A. Mosek and N. Sharon, *Infect. Immun.*, 1981, **34**, 708; (*d*) P. D. Stahl, *Curr. Opin. Immunol.*, 1992, **4**, 49; (*e*) M. E. Taylor, *Results Probl. Cell Differ.*, 2001, **33**, 105.

13 (*a*) L. Cui, J. A. Cohen, K. E. Broaders, T. T. Beaudette and J. M. Frechet, *Bioconjugate Chem.*, 2011, **22**, 949; (*b*) N. Jayaraman, K. Maiti and K. Naresh, *Chem. Soc. Rev.*, 2013, **42**, 4640; (*c*) F. Giuntini, F. Dumoulin, R. Daly, V. Ahsen, E. M. Scanlan, A. S. Lavado, J. W. Aylott, G. A. Rosser, A. Beeby and R. W. Boyle, *Nanoscale*, 2012, **4**, 2034; (*d*) L. M. Artner, L. Merkel, N. Bohlke, F. Becceren-Braun, C. Weise, J. Dernedde, N. Budisa and C. P. Hackenberger, *Chem. Commun.*, 2012, **48**, 522.

14 (*a*) E. M. Hetrick, J. H. Shin, N. A. Stasko, C. B. Johnson, D. A. Wespe, E. Holmuhamedov and M. H. Schoenfisch, *ACS Nano*, 2008, **2**, 235; (*b*) B. J. Privett, S. M. Deupree, C. J. Backlund, K. S. Rao, C. B. Johnson, P. N. Coneski and M. H. Schoenfisch, *Mol. Pharm.*, 2010, **7**, 2289; (*c*) C. Z. Chen, N. C. Beck-Tan, P. Dhurjati, T. K. van Dyk, R. A. LaRossa and S. L. Cooper, *Biomacromolecules*, 2000, **1**, 473; (*d*) C. Z. Chen and S. L. Cooper, *Biomaterials*, 2002, **23**, 3359.

15 Y. Yang, S. K. Seidlits, M. M. Adams, V. M. Lynch, C. E. Schmidt, E. V. Anslyn and J. B. Shear, *J. Am. Chem. Soc.*, 2010, **132**, 13114.

16 T. Hasegawa, T. Fujisawa, M. Numata, T. Matsumoto, M. Umeda, R. Karinaga, M. Mizu, K. Koumoto, T. Kimura, S. Okumura, K. Sakurai and S. Shinkai, *Org. Biomol. Chem.*, 2004, **2**, 3091.

17 M. Q. Zhu, L. H. Wei, M. Li, L. Jiang, F. S. Du, Z. C. Li and F. M. Li, *Chem. Commun.*, 2001, 365.

18 P. Pacher, J. S. Beckman and L. Liaudet, *Physiol. Rev.*, 2007, **87**, 315.

